

Volume change of bulk metals and metal clusters due to spin-polarization

M. Payami

Center for Theoretical Physics and Mathematics, Atomic Energy Organization of Iran,
P. O. Box 11365-8486, Tehran, Iran

The stabilized jellium model (SJM) provides us a method to calculate the volume changes of different simple metals as a function of the spin polarization, ζ , of the delocalized valence electrons. Our calculations show that for bulk metals, the equilibrium Wigner-Seitz (WS) radius, $\bar{r}_s(\zeta)$, is always an increasing function of the polarization i.e., the volume of a bulk metal always increases as ζ increases, and the rate of increasing is higher for higher electron density metals. Using the SJM along with the local spin density approximation, we have also calculated the equilibrium WS radius, $\bar{r}_s(N, \zeta)$, of spherical jellium clusters, at which the pressure on the cluster with given numbers of total electrons, N , and their spin configuration ζ vanishes. Our calculations for Cs, Na, and Al clusters show that $\bar{r}_s(N, \zeta)$ as a function of ζ behaves differently depending on whether N corresponds to a closed-shell or an open-shell cluster. For a closed-shell cluster, it is an increasing function of ζ over the whole range $0 \leq \zeta \leq 1$, whereas in open-shell clusters it has a decreasing behavior over the range $0 \leq \zeta \leq \zeta_0$, where ζ_0 is a polarization that the cluster has a configuration consistent with Hund's first rule. The results show that for all neutral clusters with ground state spin configuration, ζ_0 , the inequality $\bar{r}_s(N, \zeta_0) \leq \bar{r}_s(0)$ always holds (self-compression) but, at some polarization $\zeta_1 > \zeta_0$, the inequality changes the direction (self-expansion). However, the inequality $\bar{r}_s(N, \zeta) \leq \bar{r}_s(\zeta)$ always holds and the equality is achieved in the limit $N \rightarrow \infty$.

I. INTRODUCTION

Jellium model (JM) with spherical geometry is the simplest model used in theoretical study of simple metal clusters.¹⁻³ In the spherical JM, the ions are smeared into a uniform positive charge background sphere of density $n = 3/4\pi r_s^3$ and radius $R = (zN)^{1/3}r_s$ where z and N are the valence of the atom and the number of constituent atoms of the cluster, respectively. In the simple JM calculations the value of r_s is taken to be the bulk value of the Wigner-Seitz (WS) radius of the metal. In some calculations involving metal surfaces, one may use diffuse JM to take account of the ion relaxations at the surface of that metal.⁴ However, it is a well-known fact^{5,6} that the simple JM yields negative surface energies at high electron densities ($r_s \leq 2$), and negative bulk moduli for $r_s \approx 6$. Also, using the simple JM, it is not possible to find a realistic size and energetics for metal clusters. These drawbacks have roots in the mechanical instability^{7,8} of the simple JM system. That is, the bulk jellium system is stable only for $r_s = 4.18$. In 1990, Perdew *et al.* have introduced the stabilized jellium⁸ model (SJM) by adding two corrections to the simple JM energy. The first correction subtracts the spurious self-energy of each WS cell from the JM energy, and the second correction adds to the energy the effect of difference in the potential an electron sees from the discrete pseudoions and from the jellium background. The second correction introduces the core radius parameter, r_c , of the pseudopotential which can be adjusted in such a way that the stability of the bulk jellium system could be achieved at any observed r_s value for the valence electrons. Using the value r_c^B for the core radius (which stabilizes the unpolarized bulk system) in the SJM energy functional of a spin-polarized bulk system or a cluster, it is possible to find the equilibrium r_s value for any given spin polarization ζ .

In this paper we have calculated the changes in the equilibrium r_s values due to polarization for bulk Cs, K, Na, Li, Ga, Al, and for Cs, Na, Al clusters using the SJM in the framework of local spin density approximation (LSDA). Our calculations show that for the bulk system the volume is always an increasing function of the polarization and the increasing rate is higher for higher electron density metals. Also, we have solved the self-consistent Kohn-Sham (KS) equations⁹ for Cs, Na, and Al clusters of different sizes in the spherical SJM and obtained the equilibrium sizes of the clusters for each spin configuration consistent with Pauli's exclusion principle. The results show that in a closed-shell cluster with N total electrons and polarization ζ , the equilibrium WS radius $\bar{r}_s(N, \zeta)$ is an increasing function of ζ over the whole range $0 \leq \zeta \leq 1$ whereas, for an open-shell cluster (except for the two nearest neighbors of a closed-shell cluster), it has a decreasing behavior over $0 \leq \zeta \leq \zeta_0$, and an increasing behavior over $\zeta_0 \leq \zeta \leq 1$. Here, ζ_0 corresponds to an electronic spin configuration for which Hund's first rule is satisfied. It has been shown previously¹⁰ that this property also holds in the case of the simple JM with spherical geometry. Also, the equilibrium r_s values for a neutral cluster are found to be always smaller than that of the bulk metal with the same value of the

polarization ζ . This effect is due to the surface tension which is appreciable for small clusters. On the other hand, for an N electron neutral cluster there exists a polarization value ζ_1 , beyond which the equilibrium r_s value of the cluster exceeds the bulk r_s value of unpolarized metal. This is called self-expansion¹¹⁻¹³ and for two different neutral clusters with the same number of electrons N , the ζ_1 value of the higher electron density metal is smaller than that of the lower density metal.

The structure of this paper is as follows. In section II we first show the method by which one can calculate the changes in r_s values due to spin polarization for different bulk metals. We then explain how to apply the method to metal clusters in order to calculate the equilibrium r_s values for different spin configurations. In section III we present the results of our calculations and finally, the work is concluded in section IV.

II. CALCULATIONAL SCHEME

In the context of the SJM, the average energy per valence electron in the bulk with density parameter r_s and polarization ζ is given by¹⁴

$$\varepsilon(r_s, \zeta, r_c) = t_s(r_s, \zeta) + \varepsilon_{xc}(r_s, \zeta) + \bar{w}_R(r_s, r_c) + \varepsilon_M(r_s), \quad (1)$$

where

$$t_s(r_s, \zeta) = \frac{c_k}{r_s^2} \left[(1 + \zeta)^{5/3} + (1 - \zeta)^{5/3} \right] \quad (2)$$

$$\varepsilon_{xc}(r_s, \zeta) = \frac{c_x}{r_s} \left[(1 + \zeta)^{4/3} + (1 - \zeta)^{4/3} \right] + \varepsilon_c(r_s, \zeta) \quad (3)$$

$$c_k = \frac{3}{10} \left(\frac{9\pi}{4} \right)^{2/3}; \quad c_x = \frac{3}{4} \left(\frac{9}{4\pi^2} \right)^{1/3}. \quad (4)$$

All equations throughout this paper are expressed in Rydberg atomic units. Here t_s and ε_{xc} are the mean noninteracting kinetic energy and the exchange-correlation energy per particle, respectively. For ε_c we use the Perdew-Wang parametrization.¹⁵ Here, ε_M is the average Madelung energy, $\varepsilon_M = -9z/5r_0$, and r_0 is the radius of the WS sphere, $r_0 = z^{1/3}r_s$. We set for monovalent metals $z = 1$, and for polyvalent metals we set $z^* = 1$ (for details see Ref.[8]). In Eq.(1), $\zeta = (n_\uparrow - n_\downarrow)/(n_\uparrow + n_\downarrow)$ in which n_\uparrow and n_\downarrow are the spin densities of the homogeneous system with total density $n = n_\uparrow + n_\downarrow$. The quantity \bar{w}_R is the average value (over the WS cell) of the repulsive part of the Ashcroft empty core¹⁶ pseudopotential,

$$w(r) = -\frac{2z}{r} + w_R, \quad w_R = +\frac{2z}{r}\theta(r_c - r), \quad (5)$$

and is given by $\bar{w}_R = 3r_c^2/r_s^3$ where, z is the valence of the atom, $\theta(x)$ is the ordinary step function which assumes the value of unity for positive arguments, and zero for negative values.

The core radius is fixed to the bulk value, r_c^B , by setting the pressure of the unpolarized bulk system equal to zero at the observed equilibrium density $\bar{n} = 3/4\pi\bar{r}_s^3$:

$$\left. \frac{\partial}{\partial r_s} \varepsilon(r_s, 0, r_c) \right|_{r_s=\bar{r}_s, r_c=r_c^B} = 0. \quad (6)$$

The derivative is taken at fixed r_c , and the solution of the above equation gives r_c^B as a function of \bar{r}_s

$$r_c^B(\bar{r}_s) = \frac{\bar{r}_s^{3/2}}{3} \left\{ \left[-2t_s(r_s, 0) - \varepsilon_x(r_s, 0) + r_s \frac{\partial}{\partial r_s} \varepsilon_c(r_s, 0) - \varepsilon_M(r_s) \right]_{r_s=\bar{r}_s} \right\}^{1/2}. \quad (7)$$

Here, $\bar{r}_s \equiv \bar{r}_s(\zeta = 0)$ is the observed equilibrium density parameter for the unpolarized bulk system, and takes the values of 2.07, 2.19, 3.28, 3.99, 4.96, 5.63 for Al, Ga, Li, Na, K, Cs, respectively. Inserting the r_c^B from Eq. (7) into Eq. (1), the equilibrium r_s value of the polarized bulk system is obtained by the solution of the equation

$$\left. \frac{\partial}{\partial r_s} \varepsilon(r_s, \zeta, r_c^B) \right|_{r_s = \bar{r}_s} = 0. \quad (8)$$

The derivative is taken at fixed ζ and r_c^B . The solution gives the equilibrium density parameter $\bar{r}_s(\zeta)$ as a function of the polarization. In this procedure, by taking a constant value for the core radius of the pseudopotential, we have assumed that the core region of an atom is rigid and does not change in the process of the spin polarization of the delocalized valence electrons. This approximation works well when the distance between the neighboring atoms is sufficiently larger than the extension of the core electron orbital wave functions.

The SJM energy for a spin-polarized system with boundary surface is⁸

$$\begin{aligned} E_{\text{SJM}}[n_\uparrow, n_\downarrow, n_+] &= E_{\text{JM}}[n_\uparrow, n_\downarrow, n_+] + (\varepsilon_M(r_s) + \bar{w}_R(r_s, r_c^B)) \int d\mathbf{r} n_+(\mathbf{r}) \\ &+ \langle \delta v \rangle_{\text{WS}}(r_s, r_c^B) \int d\mathbf{r} \Theta(\mathbf{r}) [n(\mathbf{r}) - n_+(\mathbf{r})], \end{aligned} \quad (9)$$

where

$$\begin{aligned} E_{\text{JM}}[n_\uparrow, n_\downarrow, n_+] &= T_s[n_\uparrow, n_\downarrow] + E_{xc}[n_\uparrow, n_\downarrow] \\ &+ \frac{1}{2} \int d\mathbf{r} \phi([n, n_+]; \mathbf{r}) [n(\mathbf{r}) - n_+(\mathbf{r})] \end{aligned} \quad (10)$$

and

$$\phi([n, n_+]; \mathbf{r}) = 2 \int d\mathbf{r}' \frac{[n(\mathbf{r}') - n_+(\mathbf{r}')]}{|\mathbf{r} - \mathbf{r}'|}. \quad (11)$$

Here, $n = n_\uparrow + n_\downarrow$ and $\Theta(\mathbf{r})$ takes the value of unity inside the jellium background and zero, outside. The first and second terms in the right hand side of Eq.(10) are the non-interacting kinetic energy and the exchange-correlation energy, and the last term is the Coulomb interaction energy of the system. The effective potential, used in the self-consistent KS equations, is obtained by taking the variational derivative of the SJM energy functional with respect to the spin densities as

$$\begin{aligned} v_{eff}^\sigma([n_\uparrow, n_\downarrow, n_+]; \mathbf{r}) &= \frac{\delta}{\delta n_\sigma(\mathbf{r})} (E_{\text{SJM}} - T_s) \\ &= \phi([n, n_+]; \mathbf{r}) + v_{xc}^\sigma([n_\uparrow, n_\downarrow]; \mathbf{r}) + \Theta(\mathbf{r}) \langle \delta v \rangle_{\text{WS}}(r_s, r_c^B), \end{aligned} \quad (12)$$

where $\sigma = \uparrow, \downarrow$. By solving the KS equations

$$(\nabla^2 + v_{eff}^\sigma(\mathbf{r})) \phi_i^\sigma(\mathbf{r}) = \varepsilon_i^\sigma \phi_i^\sigma(\mathbf{r}), \quad \sigma = \uparrow, \downarrow, \quad (13)$$

$$n(\mathbf{r}) = \sum_{\sigma=\uparrow, \downarrow} n_\sigma(\mathbf{r}), \quad (14)$$

$$n_\sigma(\mathbf{r}) = \sum_{i(\text{occ})} |\phi_i^\sigma(\mathbf{r})|^2, \quad (15)$$

and finding the self-consistent values for ε_i^σ and ϕ_i^σ , one obtains the total energy.

In our spherical JM, we have

$$n_+(\mathbf{r}) = \frac{3}{4\pi r_s^3} \theta(R - r) \quad (16)$$

in which $R = (zN)^{1/3} r_s$ is the radius of the jellium sphere, and $n(\mathbf{r})$ denotes the electron density at point \mathbf{r} in space. The quantity $\langle \delta v \rangle_{\text{WS}}$ is the average of the difference potential over the Wigner-Seitz cell and the difference potential, δv , is defined as the difference between the pseudopotential of a lattice of ions and the electrostatic potential of the jellium positive background. Using the Eq. (21) of Ref. [8], this average value is given by

$$\langle \delta v \rangle_{\text{WS}}(r_s, r_c^B) = \frac{3(r_c^B)^2}{r_s^3} - \frac{3}{5r_s}. \quad (17)$$

Applying Eq. (9) to a metal cluster which contains N_\uparrow spin-up, N_\downarrow spin-down and $N (= N_\uparrow + N_\downarrow)$ total electrons, the SJM energy becomes a function of N , $\zeta \equiv (N_\uparrow - N_\downarrow)/N$, r_s , and r_c^B . The equilibrium density parameter, $\bar{r}_s(N, \zeta)$, for a cluster is the solution of the equation

$$\left. \frac{\partial}{\partial r_s} E(N, \zeta, r_s, r_c^B) \right|_{r_s = \bar{r}_s(N, \zeta)} = 0. \quad (18)$$

Here again, the derivative is taken at fixed values of N , ζ , and r_c^B . For an N -electron cluster, we have solved the KS equations⁹ self-consistently for various spin configurations and r_s values and obtained the equilibrium density parameter, $\bar{r}_s(N, \zeta)$, and its corresponding energy, $\bar{E}(N, \zeta) \equiv E(N, \zeta, \bar{r}_s(N, \zeta), r_c^B)$ for each allowed spin configuration.

III. RESULTS

In Fig. 1 we have shown the r_c^B values obtained from the application of Eq. (7) to different r_s values. Different metals are specified by the rigid squares. It is seen that the plot shows a linear behavior for relatively low electron density metals. Inserting these values of r_c^B into Eq. (1) and solving the Eq. (8) for different values of polarization, ζ , we have obtained the equilibrium r_s values for different bulk metals at various polarizations. The values obtained at $\zeta = 1$ are 2.62, 2.72, 3.69, 4.36, 5.28, and 5.93 for Al, Ga, Li, Na, K, and Cs, respectively. The result for all polarizations ($0 \leq \zeta \leq 1$) is shown in Fig. 2. In this figure, we have plotted the changes in the equilibrium r_s values relative to the unpolarized value as a function of the polarization for different metals. The results show an increasing behavior for all metals but, the increasing rate is higher for higher electron density metals. This property can be easily explained in terms of the Fermi holes around the electrons seen by other electrons with the same quantum numbers. In the case of very low electron density metals, the average distance between the electrons is much more larger than the effective range of the Fermi hole. Therefore, if some or all of the spin-down electrons undergo a spin flip and change to spin-up electrons, the number of spin-up electron Fermi holes will increase. But, these Fermi holes will not have any overlap and therefore, effectively no repulsive force will act on the electrons to increase the volume of the system. On the other hand, if the average distance between the electrons in a metal be much less than the range of a Fermi hole, then these spin flips cause the Fermi holes to overlap and as a result a large repulsive force will act on the electrons to increase the volume of the system. This explains the higher increasing rate for Al and the lower increasing rate for Cs metals. Figure 3 shows the plot of $\langle \delta v \rangle_{\text{WS}}(\bar{r}_s, r_c^B(\bar{r}_s))$, obtained from Eq. (17) and Eq. (7), as a function of the bulk equilibrium WS radius, \bar{r}_s . The rigid squares correspond to different metals. The value of $\langle \delta v \rangle_{\text{WS}}$ for Na is vanishingly small because, the equilibrium r_s value of sodium is very close to 4.18 at which this average vanishes. For values of r_s greater than 4.18, the correction to the KS effective potential is positive [see Eq.(12)] and this decreases the well depth and cause the electrons relax outward to make the pressure on the system (due to jellium model) to vanish. In this case, the leakage of the electrons across the jellium boundary surface is increased relative to the simple JM case. On the other hand, for $r_s < 4.18$ the potential depth is increased by the correction and the electrons should decrease their relative mean distance to make the pressure on the jellium system to vanish. Therefore, the leakage of the electrons decreases relative to the simple jellium model case. In Fig. 4, using the Eqs. (7), (8), and (17) we have plotted the variation of $\langle \delta v \rangle_{\text{WS}}(\bar{r}_s(\zeta), r_c^B)$ as a function of ζ for different metallic densities. For low electron density metals, it has a decreasing behavior and in the case of K metal, there is a change in the sign at high polarizations. However, for Al and Ga, it shows rather different behaviors. That is, all Cs, K, Na, Li show a decreasing behavior over the whole range $0 \leq \zeta \leq 1$ whereas, Al and Ga have decreasing behaviors at lower polarizations and increasing behaviors at higher polarizations. These different behaviors can be explained by the detail analysis of the Eq.(17). The right hand side of Eq.(17) has a physical minimum at $r_s = \sqrt{15}r_c^B$. In order to realize this minimum for a metal over the range $0 \leq \zeta \leq 1$, the core radius of that metal should satisfy the inequality

$$\frac{\bar{r}_s(0)}{\sqrt{15}} \leq r_c^B \leq \frac{\bar{r}_s(1)}{\sqrt{15}}. \quad (19)$$

In the above inequaty, $\bar{r}_s(0)$ and $\bar{r}_s(1)$ are the equilibrium values at $\zeta = 0$ and $\zeta = 1$, respectively. Examining for different metals show that, out of the six mentioned metals, only Al and Ga with respective core radius values of 0.56 and 0.65 satisfy this constraint. Comparing this figure with Fig. 1 of Ref. [14], reveals the different behaviors for high electron density metals, predicted by the stabilized spin-polarized jellium model¹⁴ (SSPJM). The different behavior in the SSPJM has roots in the rough estimation used there for the increment in r_s due to polarization. But here, we could calculate the increment for each metal separately, as shown in Fig. 2.

In order to find the equilibrium size of an N electron cluster in the SJM for various spin configurations of $N_\uparrow - N_\downarrow = 0$, $N_\uparrow - N_\downarrow = 2$, $N_\uparrow - N_\downarrow = 4$, \dots , $N_\uparrow - N_\downarrow = N_\uparrow$, keeping the total number of electrons, $N_\uparrow + N_\downarrow = N$, fixed; we solve the Eq. (18) using the set of self-consistent Eqs. (12)-(15). In the above we have assumed an even number of total electrons, N . For an odd number of electrons, the differences $(N_\uparrow - N_\downarrow)$ would also be odd numbers. In Figs. 5(a)-(c) we have plotted the equilibrium r_s values, $\bar{r}_s(N, \zeta)$, obtained for different spin configurations, as a function of $\zeta \equiv (N_\uparrow - N_\downarrow)/N$ for Cs, Na, and Al clusters. To clarify the different behaviors of the closed-shell and open-shell clusters, we have studied the $N=8, 20, 40$ cases which are closed-shell clusters and $N=27$ which is an open-shell cluster. We have also compared the result with the bulk case. In Figs. 5, the dashed lines correspond to the equilibrium WS radius of the unpolarized bulk metal, $\bar{r}_s(\zeta = 0)$. In all the closed-shell clusters, $\bar{r}_s(N, \zeta)$ is an increasing function of ζ while for the open-shell cluster, $N = 27$, it is decreasing over $0 \leq \zeta \leq 7/27$, and increasing over $7/27 \leq \zeta \leq 1$. Here, $\zeta_0 = 7/27$ corresponds to an electronic spin configuration for which Hund's first rule is satisfied. That is, the configuration in which the up-spin shell with $l = 3$ is half filled. This difference between closed-shell and open-shell clusters can be explained as follows. For an open-shell cluster if one increases the spin polarization from the possible minimum value consistent with the Pauli exclusion principle, one should make a spin-flip in the last incomplete shell. Because of high degeneracy for the spherical geometry, this spin-flip in the last shell does not change appreciably the kinetic energy contribution to the total energy but changes appreciably the exchange-correlation energy which in turn gives rise to a deeper effective potential that makes the KS orbitals more localized and therefore a smaller size for the cluster. On the other hand, in closed-shell clusters increasing the polarization is always accompanied by transition of electrons to unoccupied shells that have larger kinetic energies which leads to larger cluster sizes. In Figs. 5 we notice that as the size of the cluster increases, the plot of $\bar{r}_s(N, \zeta)$ resembles much more to the bulk function $\bar{r}_s(\zeta)$ and approaches to it so that, as is expected, we have

$$\lim_{N \rightarrow \infty} \bar{r}_s(N, \zeta) = \bar{r}_s(\zeta). \quad (20)$$

As we see, in all neutral clusters, the inequality

$$\bar{r}_s(N, \zeta) \leq \bar{r}_s(0) \quad (21)$$

always holds for the ground state of the cluster in which $\zeta = \zeta_0$. This effect is called self-compression¹¹ and is due to surface tension. Now if we increase the polarization of the cluster, $\zeta \equiv (N_\uparrow - N_\downarrow)/N$ relative to ζ_0 and obtain the equilibrium WS radius by solving the Eq.(18), we see that beyond some polarization, ζ_1 , the inequality in Eq.(21) changes the direction and the equilibrium r_s value of the cluster exceeds the bulk value $\bar{r}_s(0)$. This is called self-expansion which is also observed in charged metal clusters.¹² This value of ζ_1 is shifted toward zero as the size of the cluster increases. Also, comparison of Figs. 5(a)-(c) show that for two clusters with the same N , the value of ζ_1 is smaller for higher electron density metal.

In Figs. 6(a)-(c), we have plotted the quantity $\langle \delta v \rangle_{\text{WS}}$ for Cs, Na, Al clusters of different sizes, as a function of ζ , using the equilibrium values $\bar{r}_s(N, \zeta)$ in the Eq.(17); and have compared with their respective bulk functions. It is seen that for metals which the inequality in Eq.(20) does not hold, this quantity has a decreasing behavior whenever $\bar{r}_s(N, \zeta)$ has an increasing behavior, and vice versa. For Cs clusters in Fig.6(a), the quantity has positive values over the whole range $0 \leq \zeta \leq 1$. In Fig. 6(b), for Na clusters, this quantity changes sign beyond some ζ value. The Al clusters in Fig. 6(c) have negative values for $\langle \delta v \rangle_{\text{WS}}$ and they show minima as discussed before.

IV. SUMMARY AND CONCLUSION

In this work, we have calculated the equilibrium r_s values of different metals as a function of their electronic spin polarizations, using the stabilized jellium model along with the local spin density approximation. Our calculations show an increasing behavior for the bulk Wigner-Seitz radius of electron as a function of polarization. Also we have shown that the increasing rate is higher for higher electron density metals. Calculation of the equilibrium r_s values for closed-shell clusters show similar behaviors as their bulk metals i.e., they also show increasing behaviors as functions of ζ . But, the situation is somewhat different for open-shell clusters. The open-shell clusters show decreasing behavior at lower polarizations and increasing behaviors at higher polarizations. The equilibrium r_s values of the ground state configuration of the clusters are always smaller than the bulk value. This self-compression is due to the surface tension. On the other hand, at higher polarizations, the equilibrium r_s values exceeds the bulk value $\bar{r}_s(0)$, and this is called self-expansion. In conclusion, the SJM, has provided a method which can be used to calculate the sizes of the simple metal clusters with minimum possible efforts. More realistic results for open-shell clusters are possible when the spherical geometry for the jellium background is replaced by the spheroidal or ellipsoidal shapes. Work in this direction is in progress.

-
- ¹ W. E. Ekardt, Phys. Rev. B **29**, 1558 (1984).
- ² W. D. Knight, K. Clemenger, W. A. de Heer, W. A. Saunders, M. Y. Chou, and M. L. Cohen, Phys. Rev. Lett. **52**, 2141 (1984).
- ³ M. Brack, Rev. Mod. Phys. **65**, 677 (1993), and references therein.
- ⁴ A. Rubio, L. C. Balbás, and J. A. Alonso, Z. Phys. D**19**, 93 (1991).
- ⁵ N. D. Lang and W. Kohn, Phys. Rev. B **1**, 4555 (1970).
- ⁶ N. W. Ashcroft and D. C. Langreth, Phys. Rev. **155**, 682 (1967).
- ⁷ H. B. Shore and J. H. Rose, Phys. Rev. B **59**, 10485 (1999) and references therein.
- ⁸ J. P. Perdew, H. Q. Tran, and E. D. Smith, Phys. Rev. B **42**, 11627 (1990).
- ⁹ W. Kohn and L. J. Sham, Phys. Rev. **140**, A1133 (1965).
- ¹⁰ M. Payami, J. Chem. Phys. **111**, 8344 (1999).
- ¹¹ J. P. Perdew, M. Brajczewska, and C. Fiolhais, Solid State Commun. **88**, 795 (1993).
- ¹² M. Brajczewska, A. Vieira, C. Fiolhais, and J. P. Perdew, Prog. Surf. Sci. **53**, 305 (1996).
- ¹³ A. Vieira, M. B. Torres, C. Fiolhais, and L. C. Balbás, J. Phys. B: At. Mol. Opt. Phys. **30**, 3583 (1997).
- ¹⁴ M. Payami and N. Nafari, J. Chem. Phys. **109**, 5730 (1998).
- ¹⁵ J. P. Perdew and Y. Wang, Phys. Rev. B **45**, 13244 (1992).
- ¹⁶ N. W. Ashcroft, Phys. Lett. **23**, 48 (1966).

FIG. 1. The pseudopotential core radius, r_c^B , in atomic units as a function of the equilibrium r_s value of the bulk metal. The rigid squares specify different metals. The plot shows a linear behavior at rather low densities.

FIG. 2. The changes in the equilibrium WS radius relative to the unpolarized value, $[\bar{r}_s(\zeta) - \bar{r}_s(0)]$, in atomic units, for different metals as functions of the polarization, ζ . All have increasing behaviors and the increasing rate is higher for higher electron density metals.

FIG. 3. The average value of the difference potential, in Rydbergs, as a function of the equilibrium WS radius for a bulk jellium system. The rigid squares correspond to different metals.

FIG. 4. The average values of the difference potential, in Rydbergs, as functions of the polarization for different bulk metals. The plots show decreasing behaviors for Cs, K, Na, Li over the whole range; whereas the plots for Ga and Al show decreasing behaviors at low polarizations, and increasing behaviors at higher polarizations with minima in between.

FIG. 5. The equilibrium WS radius, $\bar{r}_s(N, \zeta)$, in atomic units, as functions of the polarization for (a)- Cs, (b)- Na, (c)- Al clusters. In all closed-shell clusters (here, $N=8,20,40$) $\bar{r}_s(N, \zeta)$ is an increasing function of ζ while for the open-shell cluster (here, $N = 27$) it is decreasing over $0 \leq \zeta \leq 7/27$, and increasing over $7/27 \leq \zeta \leq 1$. The solid lines correspond to the bulk $\bar{r}_s(\zeta)$, and the dashed lines correspond to the equilibrium value of the unpolarized bulk system, $\bar{r}_s(0)$.

FIG. 6. The average values of the difference potential, in Rydbergs, as functions of the spin configurations, ζ . In (a)- Cs and (b)- Na, for the closed-shell clusters (here, $N=8,20,40$) it shows a decreasing behavior over the whole range, the same as the bulk case which is specified by a solid line. But, in open-shell clusters (here, $N = 27$) it is increasing over $0 \leq \zeta \leq 7/27$, and decreasing over $7/27 \leq \zeta \leq 1$. In (c)- Al, the same behaviors hold for lower polarizations but, as discussed in the text, it shows a minimum at higher polarizations.

Fig. 1, M. Payami

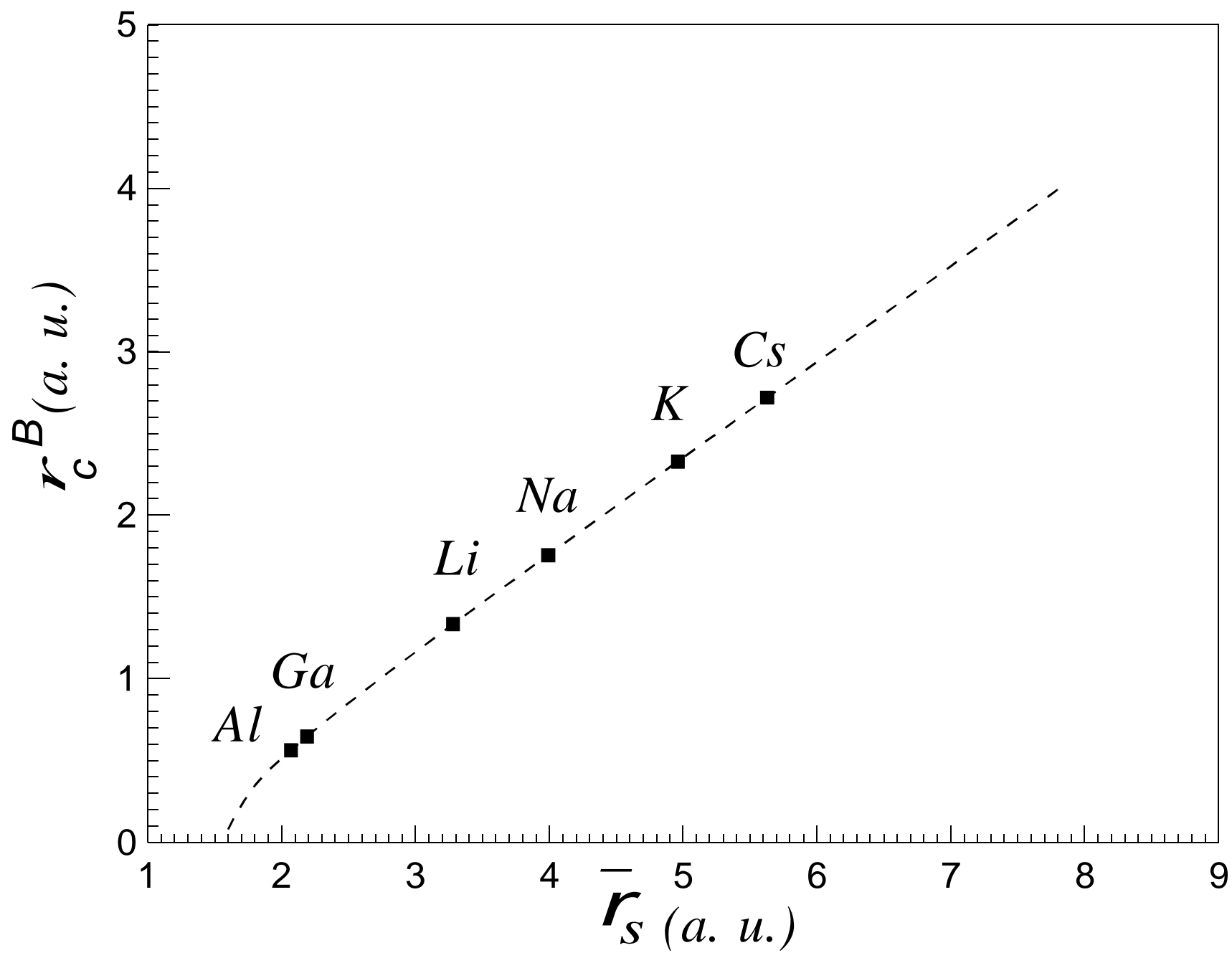


Fig2, M.Payami

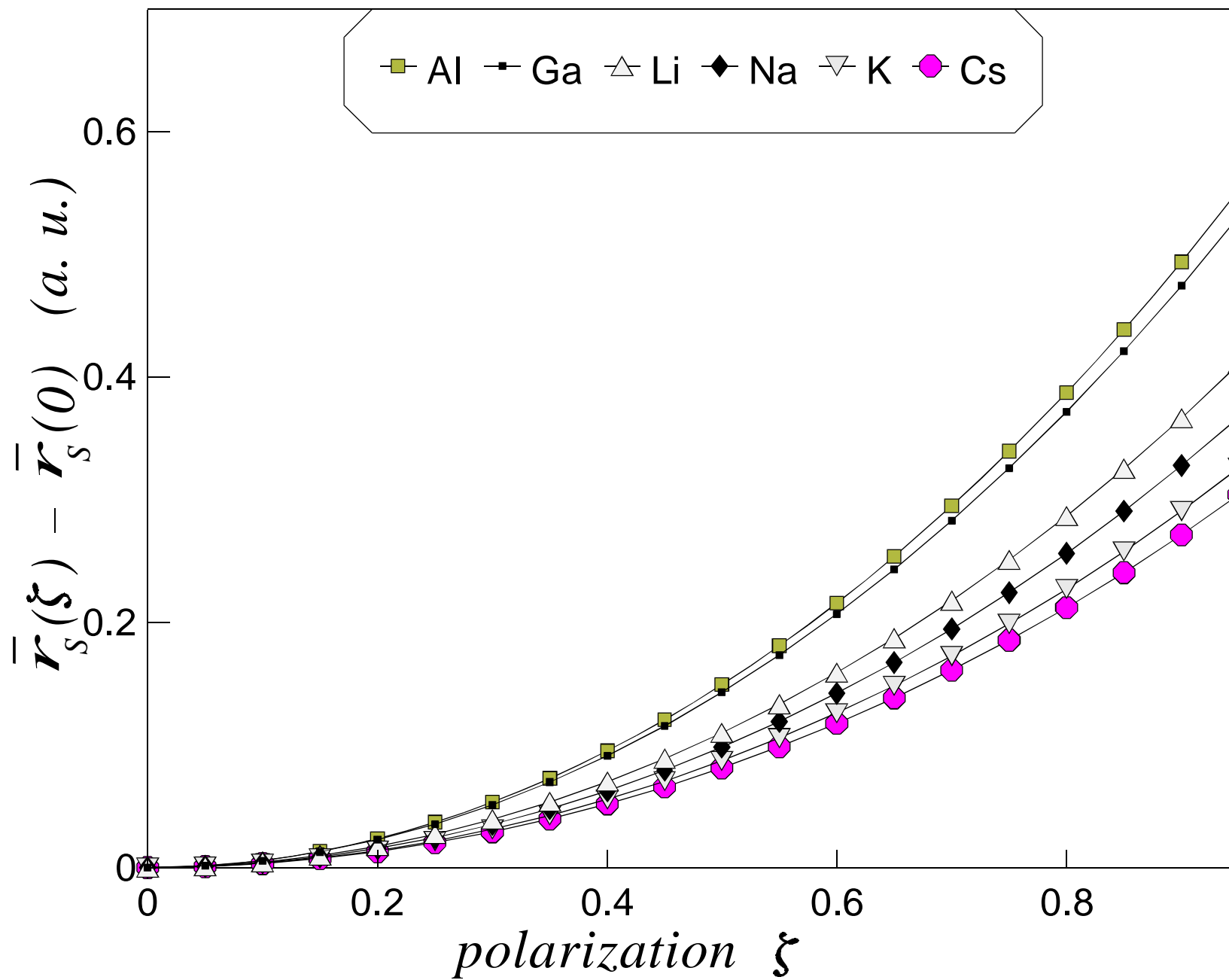


Fig3, M.Payami

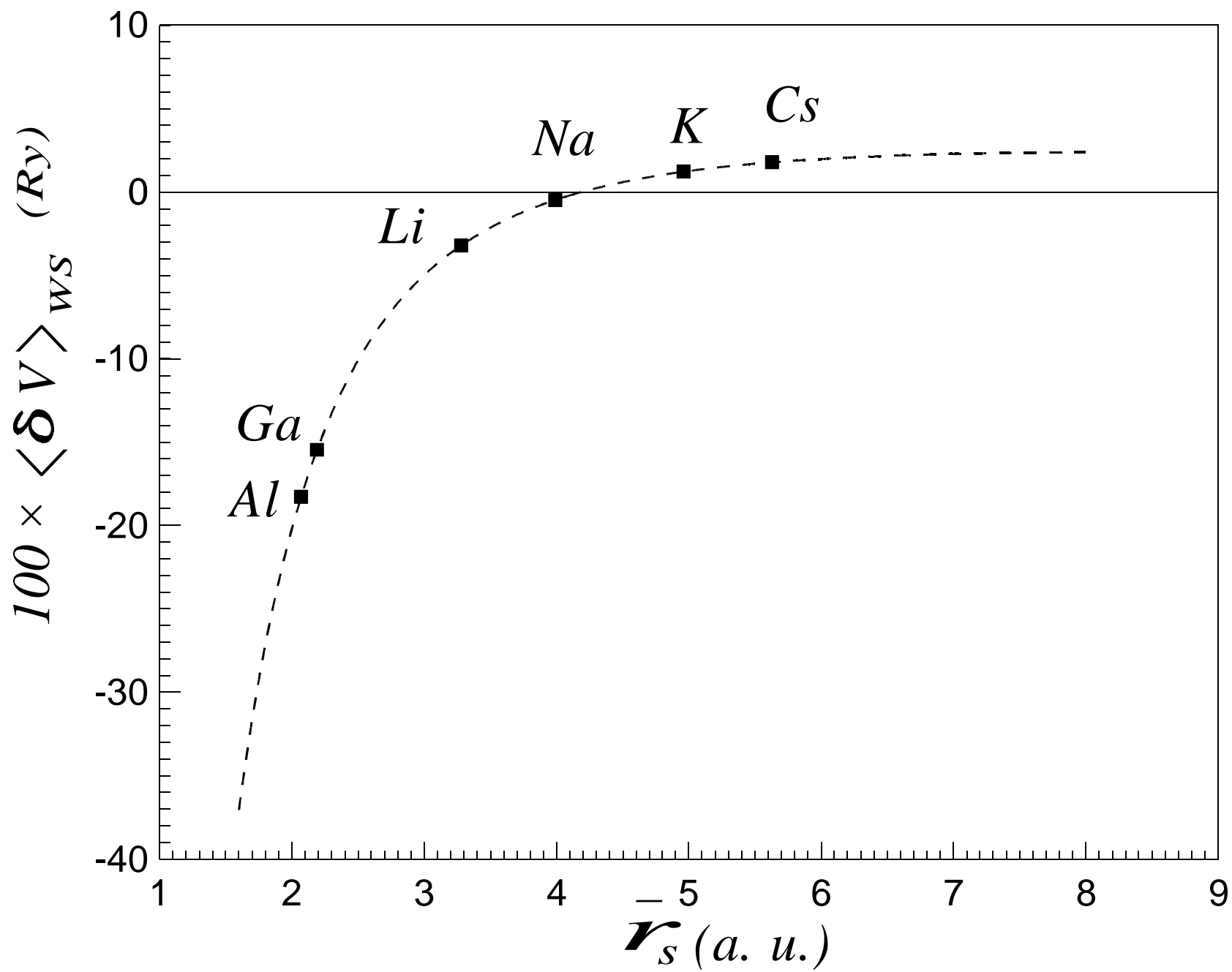


Fig4, M.Payami

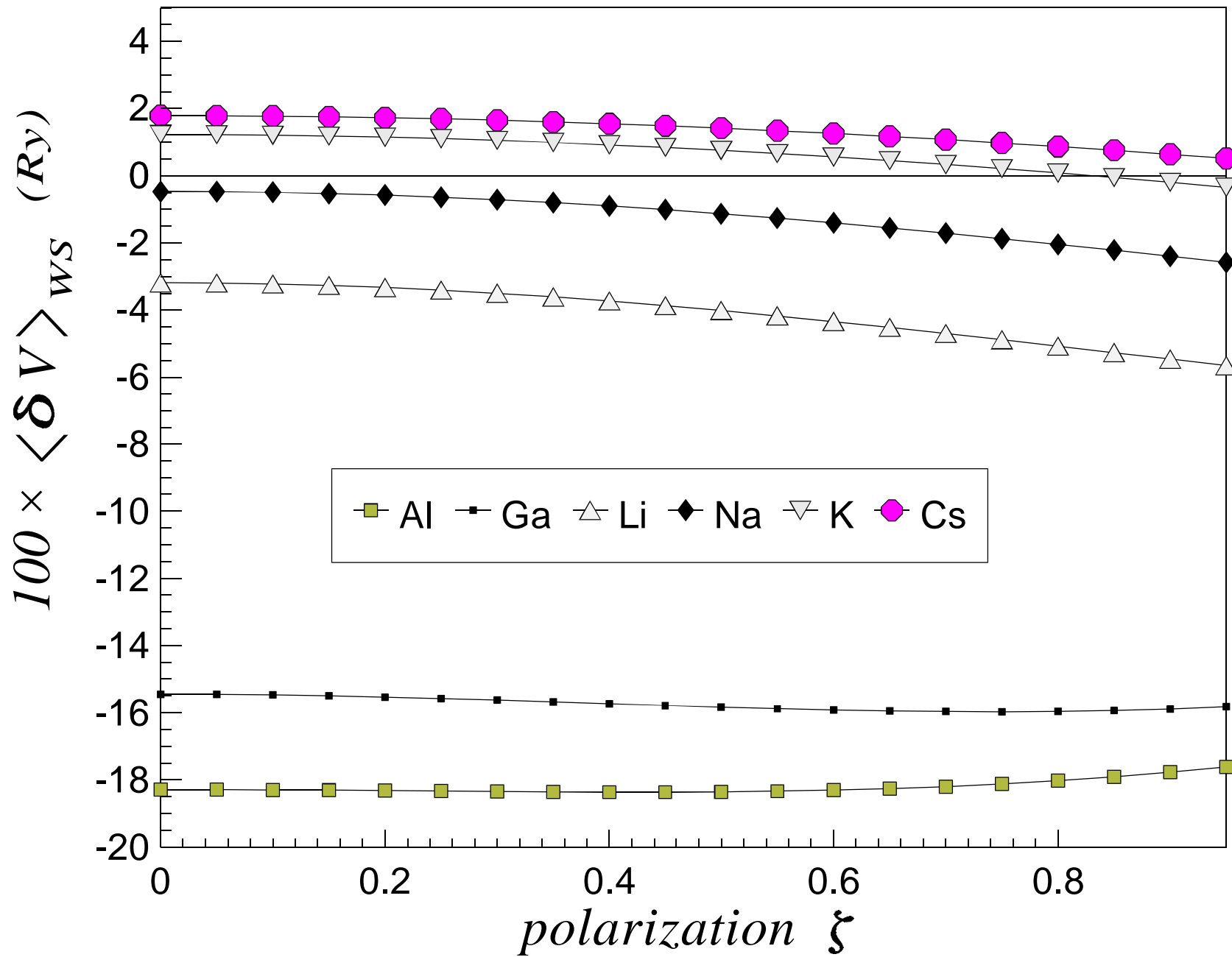


Fig5(a), M.Payami

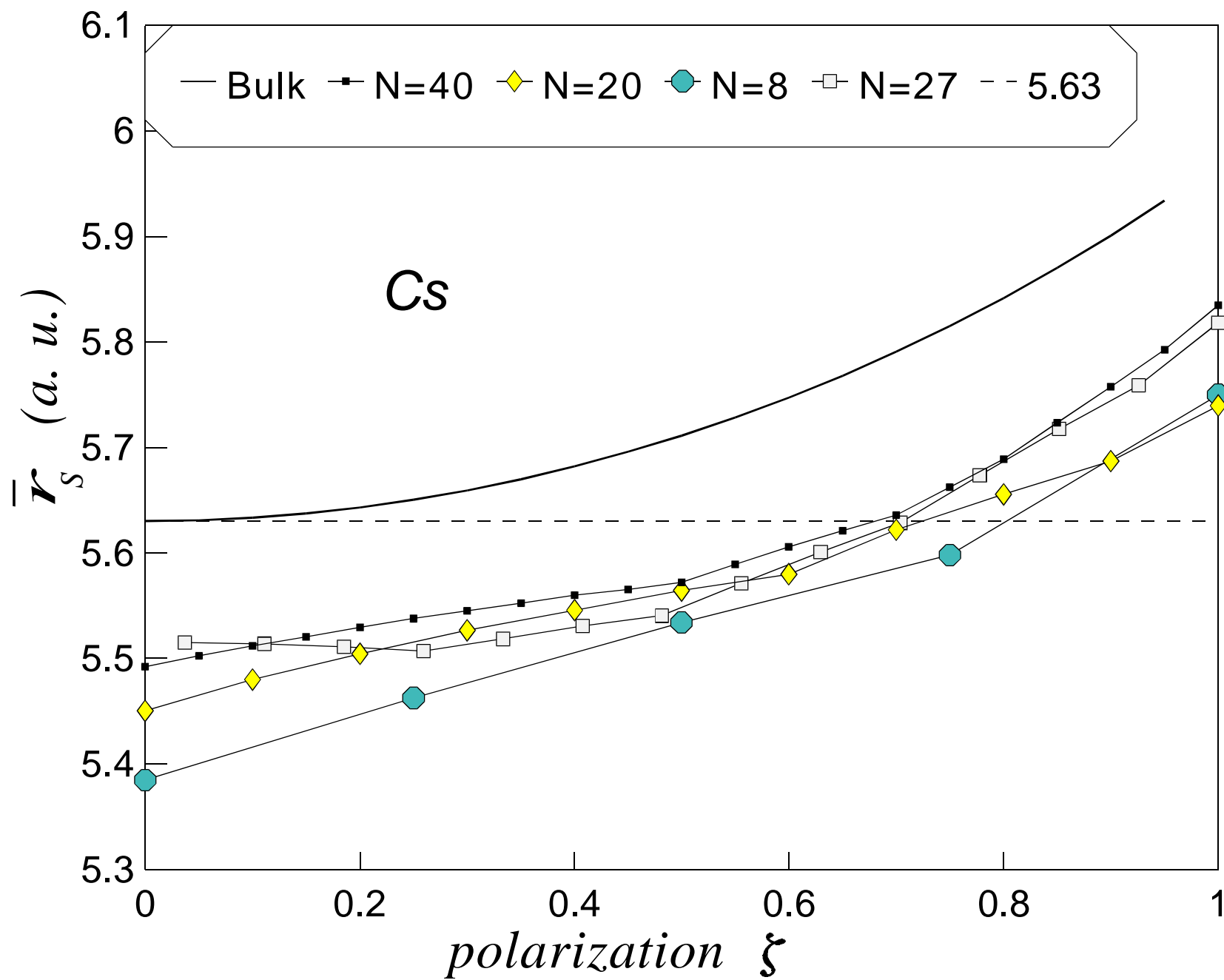


Fig5(b), M.Payami

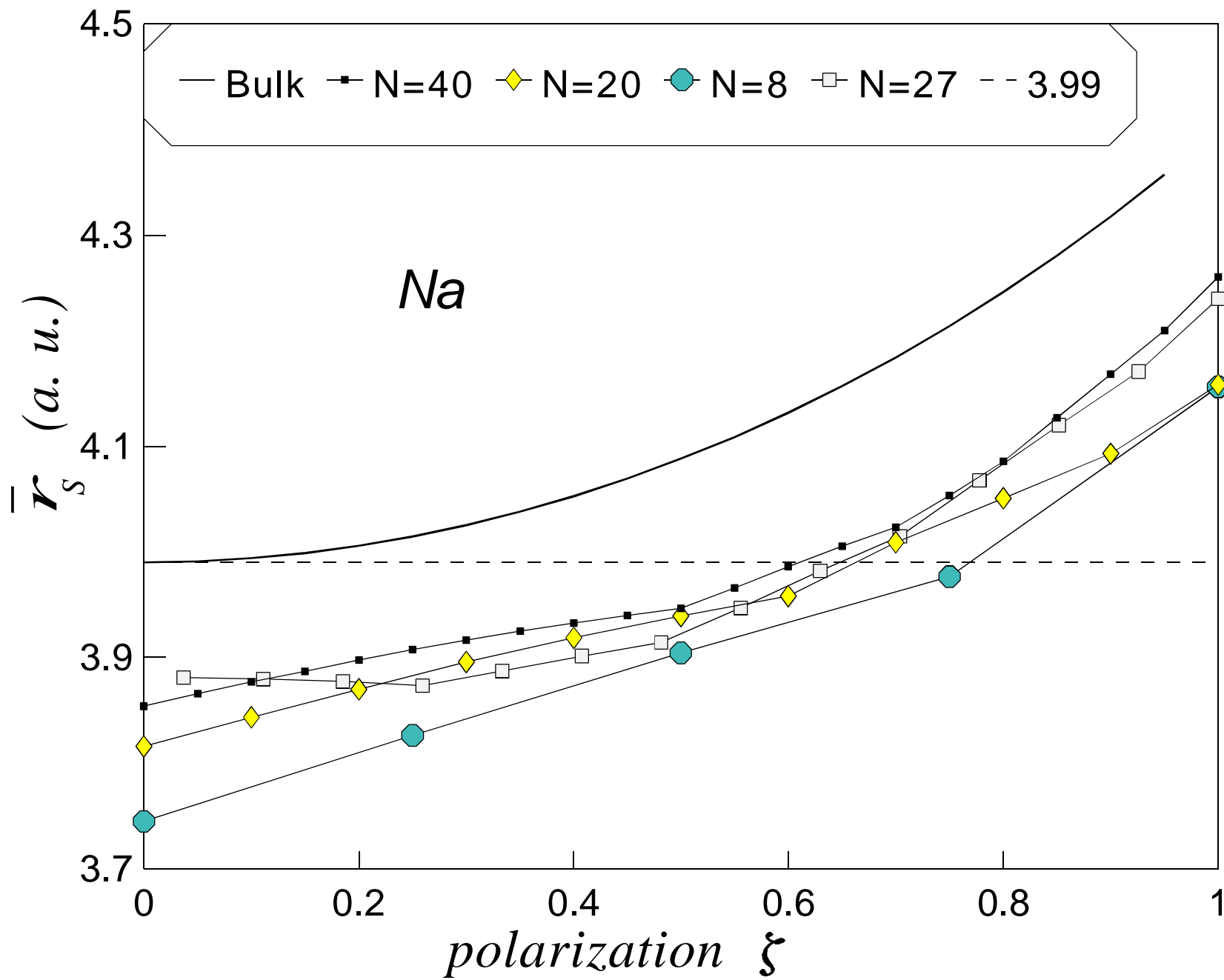


Fig5(c), M.Payami

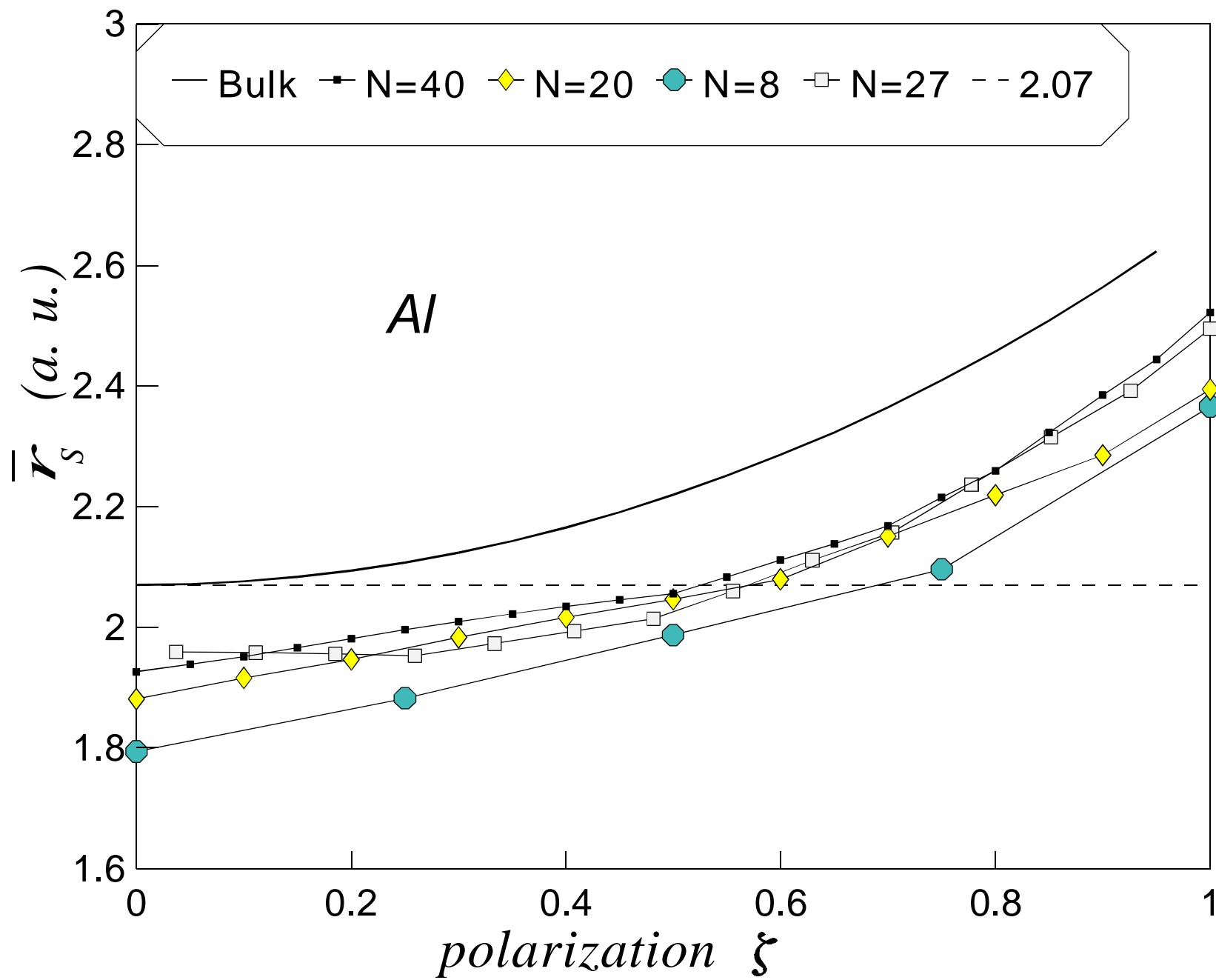


Fig6(a), M.Payami

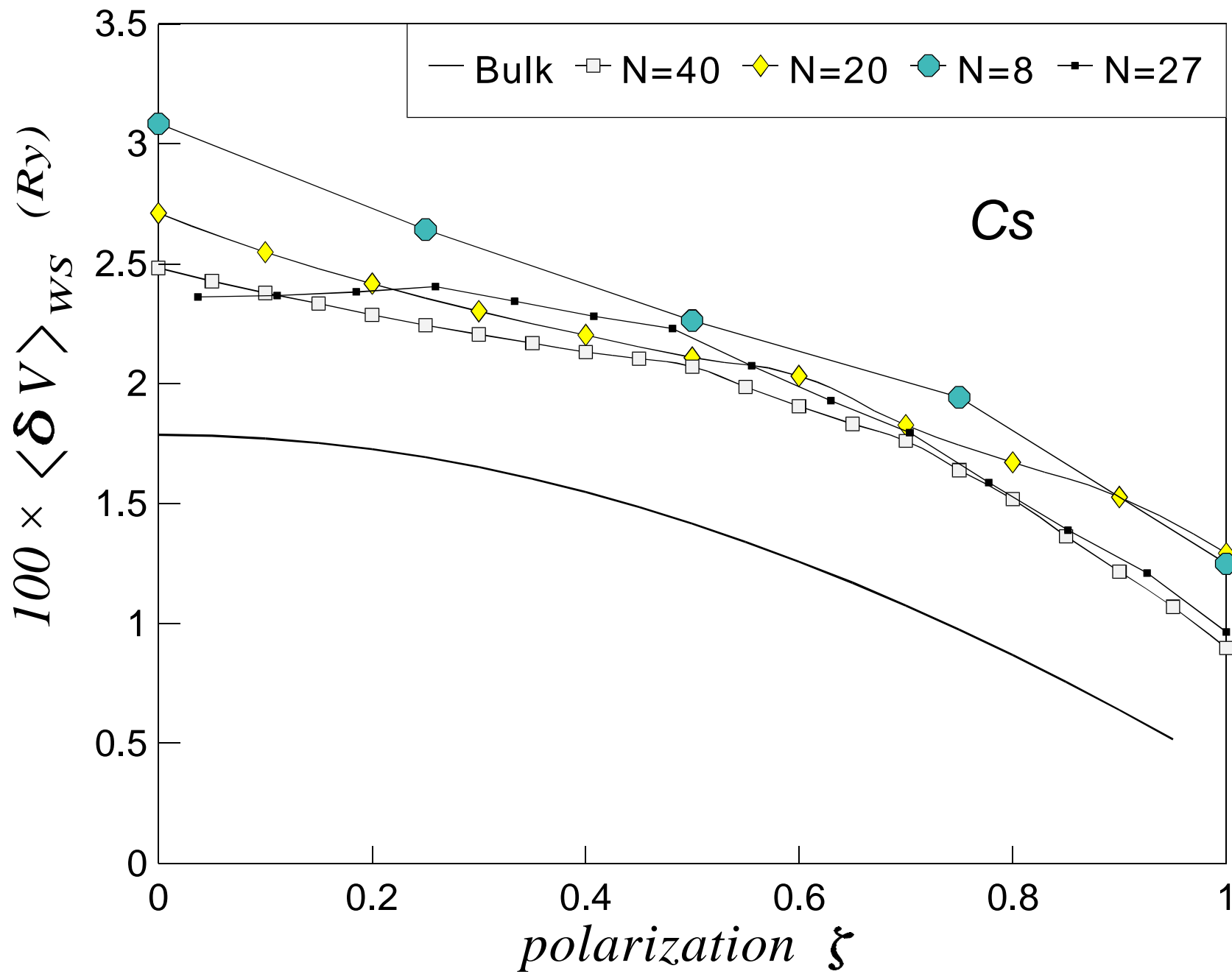


Fig6(b), M.Payami

